Journal of Advanced Research in Science and Technology
ISSN: 2352-9989

Direct power control based artificial neural networks of doubly fed induction generator for wind energy conversion system application

Youcef Djeriri [1*]
Department of Electrical Engineering, University Djillali Liabes of Sidi Bel Abbes, Algeria, 22000
ICEPS (Intelligent Control & Electrical Power Systems) laboratory

Abstract. This paper proposes a Direct Power Control (DPC) strategy for a Doubly Fed Induction Generator (DFIG) based wind power generation system, using a Multilayer Perceptron (MLP) controller. This controller replaces the conventional DPC lookup table and allows the converter that is connected to the rotor terminals to operate with constant switching frequency. The digital simulation results of 1.5 MW DFIG are presented to show the validity and efficiency of the proposed control strategy to decouple and control the active and reactive power in different conditions of wind speed.

Keywords: *Wind energy, Doubly fed induction generator, Direct power control, Artificial neural networks, Multilayer perceptron.*

1. Introduction

Nowadays, the concept of the variable speed wind turbine (VSWT) equipped with a Doubly Fed Induction Generator (DFIG) has received increasing attention due to its noticeable advantages compared to the fixed speed induction generators [1–2], such as increased power capture, four-quadrant converter topology which lets the decoupled and fast active and reactive power control and reduced mechanical stresses [3].

In the DFIG concept, the stator is usually connected directly to the three-phase grid; the rotor is also connected to the grid but through a transformer and a variable frequency converter as shown in the Fig. 1. This arrangement provides flexibility of operation in sub-synchronous and super-synchronous speeds in both generating and motoring modes (± 30 % around the synchronous speed). By consequence, the power converter needs to handle a fraction (20 – 30 %) of the total power to achieve full control of the generator. Such the system also results in lower converter costs and lower power losses compared to fully variable speed wind generation systems with a full-rated converter.

Recently, Direct Power Control (DPC) of DFIG based wind energy generation systems has been proposed [4–5], and it's proven to have many advantages compared to the vector control technique, such as simplicity, fast dynamics and robustness against parameters variations and grid disturbances [6]. However, when DPC operate at a variable switching frequency [6–7], its makes the power converter and the AC harmonic filter complicated and expensive. More recently, several papers have been published on DPC at constant switching frequency for DFIG, proposing new modified DPC strategies and improvements of the system [8, 9, 10, 11, 12, 13].

* Corresponding author.
E-mail: youcef.djeriri@univ-sba.dz (Djeriri Y.).
Address: University Djillali Liabes of Sidi Bel Abbes, Algeria.

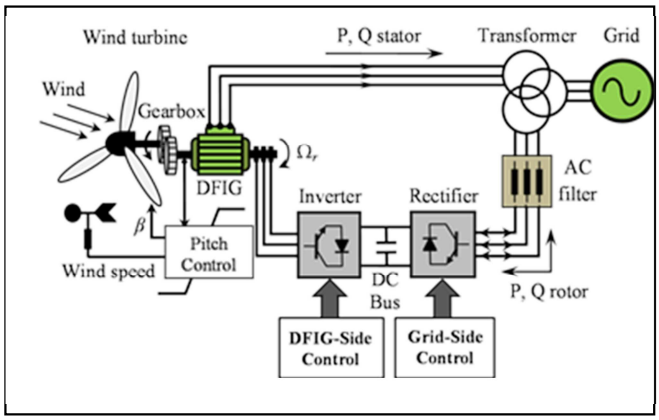

Fig. 1: WECS based a DFIG configuration

In this paper a DPC with constant switching frequency was proposed, which allows the performance of DPC scheme in terms of active and reactive power ripples and current distortion to be improved. These improvements could be achieved with simple control circuit without increasing the inverter switching frequency. This control algorithm is based on an Artificial Neural Networks (ANNs) with the multilayer perceptron (MLP) structure. By suitable selection of the best structure of MLP, the complexity of the proposed method is less than the method presented by [14].

2. Dynamic of the DFIG

For decoupled control of active and reactive power, dynamic model of DFIG is required

The voltage equations of the DFIG in the synchronous *d-q* reference frame rotating at ω_s are as follows:

$$V_{ds} = R_s I_{ds} + \frac{d}{dt}\psi_{ds} - \omega_s \psi_{qs} \quad (1)$$

$$V_{qs} = R_s I_{qs} + \frac{d}{dt}\psi_{qs} + \omega_s \psi_{ds} \quad (2)$$

$$V_{dr} = R_r I_{dr} + \frac{d}{dt}\psi_{dr} - (\omega_s - \omega_r)\psi_{qr} \quad (3)$$

$$V_{qr} = R_r I_{qr} + \frac{d}{dt}\psi_{qr} + (\omega_s - \omega_r)\psi_{dr} \quad (4)$$

Where:

ω_s : stator angular frequency in rad/s

ω_r : rotor angular speed in rad/s

$(\omega_s - \omega_r)$: slip angular frequency in rad/s

The flux linkages are :

$$\psi_{ds} = L_s I_{ds} + L_m I_{dr} \quad (5)$$

$$\psi_{qs} = L_s I_{qs} + L_m I_{qr} \quad (6)$$

$$\psi_{dr} = L_r I_{dr} + L_m I_{ds} \tag{7}$$

$$\psi_{qr} = L_r I_{qr} + L_m I_{qs} \tag{8}$$

DFIG electromagnetic torque is:

$$T_{em} = \frac{3}{2} p \frac{L_m}{L_r} \left(\psi_{qs} I_{dr} - \psi_{ds} I_{qr} \right) \tag{9}$$

Generator active and reactive powers at the stator side are given by the following expressions:

$$P_s = \frac{3}{2} \left(V_{ds} I_{ds} + V_{qs} I_{qs} \right) \tag{10}$$

$$Q_s = \frac{3}{2} \left(V_{qs} I_{ds} - V_{ds} I_{qs} \right) \tag{11}$$

The rotor-side converter is controlled in a synchronously rotating *d-q* axis frame, with the d-axis oriented along the stator flux vector position (Fig. 2). In this approach, decoupled control between the stator active and reactive powers is obtained. The influence of the stator resistance can be neglected and the stator flux can be held constant as the stator is connected to the grid [5]. Consequently [15]:

$$\psi_{ds} = \psi_s \text{ and } \psi_{qs} = 0 \tag{12}$$

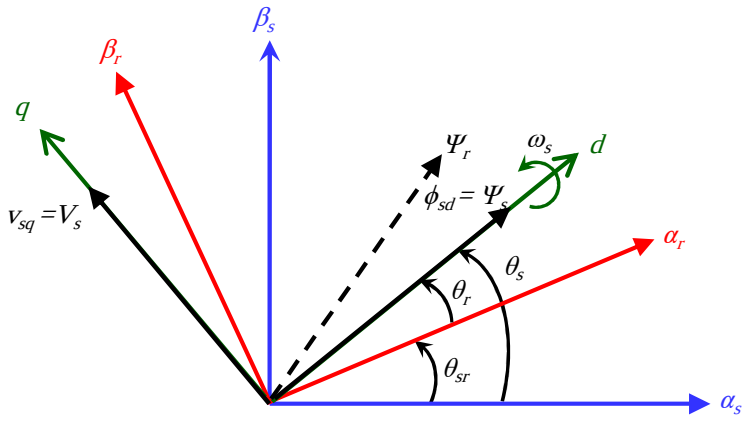

Fig. 2: Stator field oriented control technique

In this case :

$$\begin{cases} V_{ds} = 0 \\ V_{qs} = V_s = \omega_s . \psi_s \end{cases} \tag{13}$$

$$\begin{cases} \psi_s = L_s I_{ds} + L_m I_{dr} \\ 0 = L_s I_{qs} + L_m I_{qr} \end{cases} \tag{14}$$

$$\begin{cases} I_{ds} = \dfrac{\psi_s}{L_s} - \dfrac{L_m}{L_r} I_{dr} \\ I_{qs} = -\dfrac{L_m}{L_s} I_{qr} \end{cases} \tag{15}$$

$$\begin{cases} P_s = \dfrac{3}{2} V_s I_{qs} \\ Q_s = \dfrac{3}{2} V_s I_{ds} \end{cases} \tag{16}$$

Replacing the stator currents by their expressions given in (5) and (6), the equations below are expressed:

$$\begin{cases} P_s = -\dfrac{3}{2}\dfrac{L_m}{L_s} V_s I_{qr} \\ Q_s = \dfrac{3}{2} V_s \left(\dfrac{V_s}{L_s.\omega_s} - \dfrac{L_m}{L_s} I_{dr} \right) \end{cases} \tag{17}$$

The electromagnetic torque is as follows:

$$T_{em} = -\frac{3}{2} p \frac{L_m}{L_s} \psi_s I_{qr} \tag{18}$$

Rotor voltages can be expressed by:

$$\begin{cases} V_{dr} = R_r I_{dr} - g\omega_s \left(L_r - \dfrac{{L_m}^2}{L_s} \right) I_{qr} \\ V_{qr} = R_r I_{qr} + g\omega_s \left(L_r - \dfrac{{L_m}^2}{L_s} \right) I_{dr} + g \dfrac{L_m V_s}{L_s} \end{cases} \tag{19}$$

3. Conventional DPC strategy principle

By using pervious equations and neglecting the stator resistance; we can find the relations of P_s and Q_s according to both components of the rotor flux in the stationary $(\alpha_r\text{-}\beta_r)$ reference frame, and we can get:

$$\begin{cases} P_s = -\dfrac{3}{2}\dfrac{L_m}{\sigma L_s L_r} V_s \psi_{\beta r} \\ Q_s = \dfrac{3}{2} V_s \left(\dfrac{1}{\sigma L_s} \psi_s - \dfrac{L_m}{\sigma L_s L_r} \psi_{\alpha r} \right) \end{cases} \tag{20}$$

Where:

$$\begin{cases} \psi_{\alpha r} = \left(L_r - \dfrac{L_m^{\,2}}{L_s} \right) I_{\alpha r} + \dfrac{L_m}{L_s} \psi_s \\ \psi_{\beta r} = \left(L_r - \dfrac{L_m^{\,2}}{L_s} \right) I_{\beta r} \\ \sigma = \left(L_s L_r - L_m^2 \right) / L_s L_r \end{cases} \tag{21}$$

The fact that the stator is directly connected to the grid provides a stator flux vector with constant amplitude:

$$\left| \overline{\psi}_s \right| = \frac{\left| \overline{V}_s \right|}{\omega_s} \tag{22}$$

If we introducing the angle δ between the rotor and stator flux linkage, P_s and Q_s become:

$$\begin{cases} P_s = -\dfrac{3}{2} \dfrac{L_m}{\sigma L_s L_r} \omega_s |\psi_s| |\psi_r| \sin\delta \\ Q_s = \dfrac{3}{2} \dfrac{\omega_s}{\sigma L_s} |\psi_s| \left(\dfrac{L_m}{L_r} |\psi_r| \cos\delta - |\psi_s| \right) \end{cases} \tag{23}$$

Differentiating (23) results in the following equations:

$$\begin{cases} \dfrac{dP_s}{dt} = -\dfrac{3}{2} \dfrac{L_m \omega_s}{\sigma L_s L_r} |\psi_s| \dfrac{d\left(|\psi_r| \sin\delta \right)}{dt} \\ \dfrac{dQ_s}{dt} = \dfrac{3}{2} \dfrac{L_m \omega_s}{\sigma L_s L_r} |\psi_s| \dfrac{d\left(|\psi_r| \cos\delta \right)}{dt} \end{cases} \tag{24}$$

Hence, the last two expressions show that the stator active and reactive powers can be controlled by modifying the relative angle between the rotor and stator flux space vectors and their amplitudes.

4. DPC based artificial neural networks

In this study we have used a feed forward neural network to select the voltage vector which replaces the lookup table in the case of the conventional DPC strategy (Fig. 3).

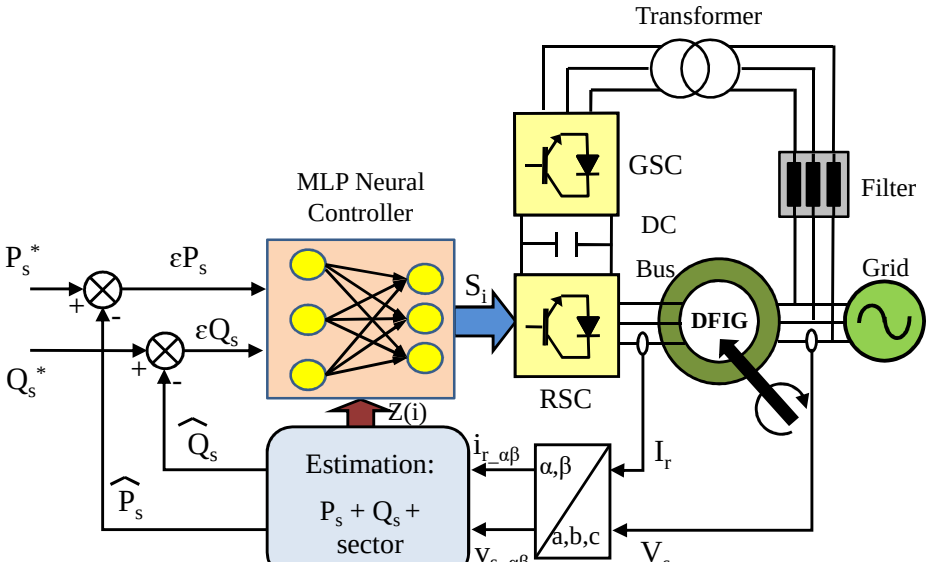

Fig. 3: DPC neural networks controller scheme

ANNs has been devised having as inputs the active power error, the reactive power error and the position of the flux sector and as output the gate pulses for the tow levels voltage source inverter (2L-VSI) which supplies the rotor windings (RSC) as it is illustrated in Fig. 4.

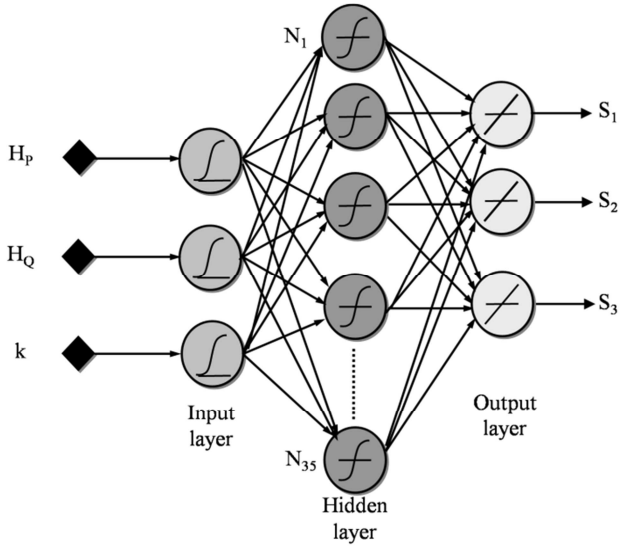

Fig. 4: Proposed MLP-ANN controller

The network taken in this study is a 3–35–3 feed–forward network with first layer of log sigmoid transfer function, second layer of hyperbolic tangent sigmoid transfer function and third layer of linear transfer function. Levenberg–Marquardt back–propagation algorithm [16–17] is used to train (updates weights and bias) this neural network at a sampling time of 10 μs.

5. Simulation results

In this part, simulations are investigated with a 1.5MW DFIG connected to a 398V/50Hz grid (appendix), by using the MATLAB/SIMULINK software. The proposed control strategy (ANN-DPC) is simulated and tested in both cases: fixed wind speed, and variable wind speed.

5.1. Fixed wind speed

In this case, the wind speed is maintained constant at its nominal value (12.25m/s), we initial simulation with various active and reactive powers steps in nominal regime of DFIG. The negative sign "-" refers to the generation of active power and to the absorption of reactive power. The DFIG is

driven from the sub-synchronous speed (1000rpm) to the super-synchronous speed (2000rpm) by crossing the synchronous speed (1500rpm). The sampling period of the system is 10µs.

All simulation results are show in Fig. 5, from top to bottom; the curves are active power (P_s), reactive power (Q_s), power factor (PF), stator currents and rotor currents.

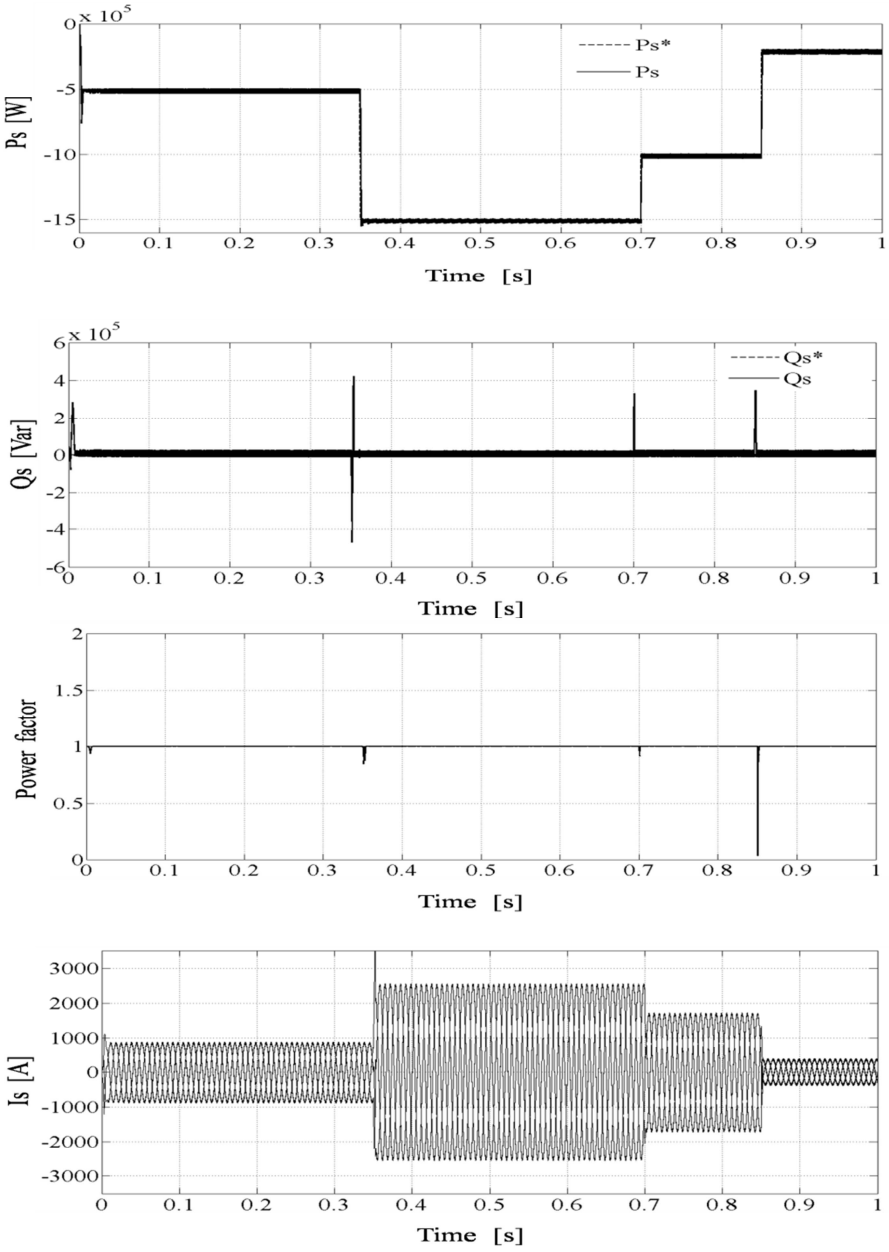

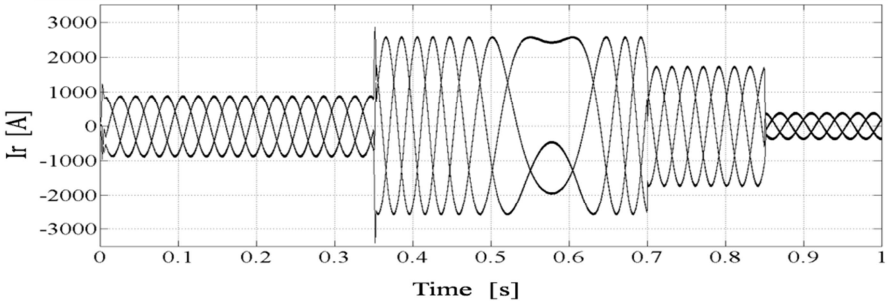

Fig. 5: ANN-DPC strategy simulation results in fixed wind speed operation

The simulation results in Fig. 5, under nominals conditions of operation show that the designed ANN-based DPC strategy is able to provide good performance. The decoupled control of active and reactive power is achieved and powers responses follow their reference values well.

The reactive power reference will be set to zero (Q_s^*=0MVAR) to ensure a unity power factor (PF=1) at the grid side, in order to optimize the generated stator active power quality. By consequence, the stator current has a negligible ripple and a nearly sinusoidal wave. In the other hand, the changeover from sub-synchronous to super-synchronous speed crossing the synchronous speed is observed to be smooth without any transients in the rotor current waveform.

5.2. Variable wind speed

In this section, simulations are performed with a varibale wind speed, with a mean value of 8.2m/s. In this case, a battery storage unit is included to the DC bus to provide a constant active power to the grid for all wind conditions. In high wind speed conditions, the DFIG provides energy to the network and refills the storage unit whereas in insufficient wind conditions, the storage unit allows compensating the lack of energy. This is a very useful operation for wind turbine grid connection.

The pitch control achieves the maximum efficiency of the turbine. It is also possible to turn off the turbine when wind speed is too large to prevent any mechanical damage. For a given wind speed, the power reference is calculated and subtracted from the constant power injected to the grid to fix the power reference for the storage unit. This power can be positive or negative according to wind speed conditions.

The power can be positive or negative if the generator performs at hyper or hypo synchronous conditions and when the storage unit absorbs power from the wind turbine or provides power to the grid.

The storage unit is controlled in power for charge and discharge, and the power stored in the battery is calculated by:

$$P_{stored} = P_s - 0.75\,MW \tag{25}$$

And the power injected to the grid is given by the expression:

$$P_{grid} = P_s^* - P_{stored} \tag{26}$$

Where P_s and P_s^* are the produced and reference active power respectively.

Fig. 6 present simulation results for a 1.5MW DFIG associated with a 0.75MW storage unit. The wind turbine is also supposed to inject a constant power of 0.75MW into the grid for all wind conditions. The ANN-DPC strategy is always simulated at 10µs sampling period.

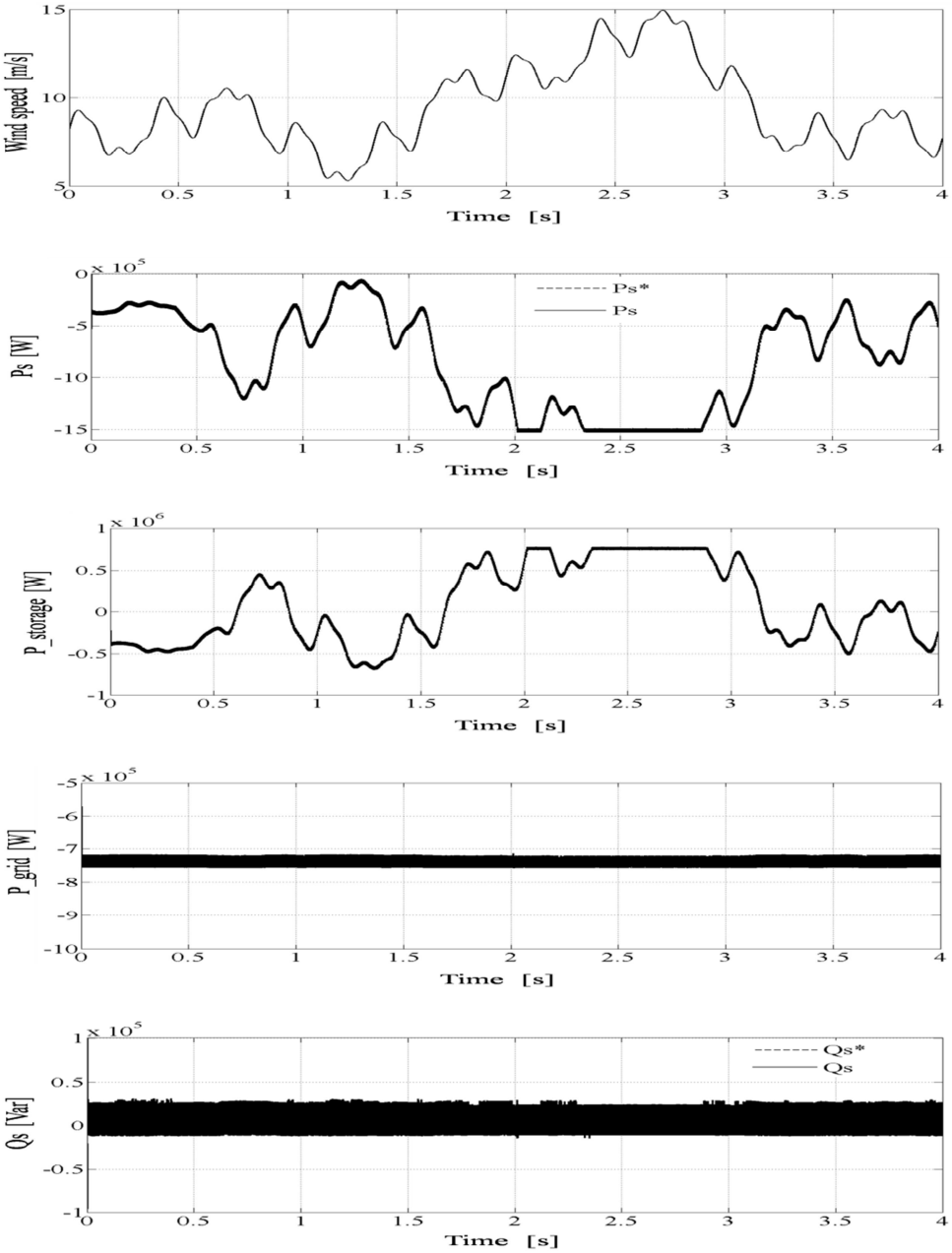

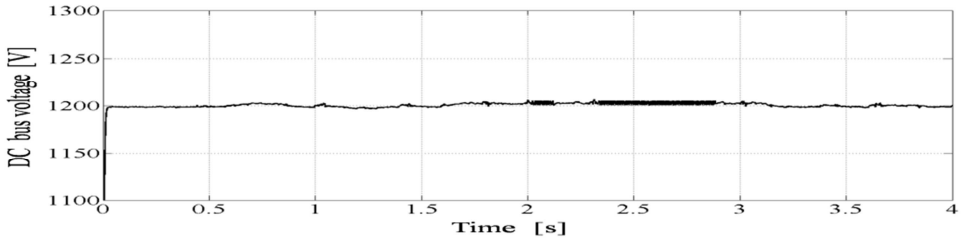

Fig. 6: ANN-DPC strategy simulation results in variable wind speed operation

In the Fig. 6, the active power of the DFIG follows the power reference calculated from the wind speed. This power is limited by the generator nominal power (1.55MW). Simulation results for active power of the DFIG demonstrate the impossibility of generating a constant active power equal to 0.75MW under all wind speed conditions. For this reason, batteries are included to maintain a constant active power at the grid side; so batteries correspond to a positive power when charging and a negative power when feeding the grid.

The produced active power is kept constant (0.75MW) for all wind conditions. This corresponds to the sum of the DFIG and storage unit powers. Consequently, this wind energy conversion system can be assimilated as a constant generator for active power.

The reactive power is correctly regulated and it's always maintained to zero with an aim of keeping a unit power factor at the grid side.

6. Conclusion

In this paper, a direct power control strategy using a controller based on artificial neural networks has been presented. This technique has been used for reference tracking and decoupling of active and reactive powers exchanged between the stator of the DFIG and the grid by the direct manipulation of rotor voltages without the need for current controllers and requiring only a single controller.

The simulation results have shown the effectiveness of the proposed strategy in attending changes of the active and reactive power with good performances at variable wind speed.

In this case, the incorporation of batteries or other energy storage device in the DC-link must be necessary to enables a temporary storage of energy and therefore, the ability to provide constant active power injected to the grid, which is both deterministic and resistant to wind speed fluctuations.

References

[1] A. Petersson, Analysis, modeling and control of doubly fed induction generators for wind turbines, PhD. thesis, Champers University of Technology, Sweden, 2005.

[2] S. EL Aimani, B, François, F. Minne, and B. Robyns, Modelling and simulation of doubly fed induction generators for variable speed wind turbines integrated in a distribution network" 10th European conference on power electronics and applications, Toulouse, France, 2-4 September 2003.

[3] L.M. Fernandez, C.A. Garcia, F. Jurado, Comparative study on the performance of control systems for doubly fed induction generator (DFIG) wind turbines operating with power regulation. Elsevier, Energy, 2008, vol. 33, pp. 1438-1452.

[4] R. Datta, V. T. Ranganathan, Direct power control of grid-connected wound rotor induction machine without rotor position sensors, IEEE Trans. Power Electron, vol. 16, no. 3, pp. 390-399, May 2001.

[5] L. Xu, P. Cartwright, Direct active and reactive power control of DFIG for wind energy generation, IEEE Trans. Energy Convers, vol. 21, no. 3, pp.750-758, Sept. 2006.
[6] Y. Djeriri, A. Meroufel, A. Massoum and Z. Boudjema, A comparative study between field oriented control strategy and direct power control strategy for DFIG, Journal of Electrical Engineering, JEE, Romania, vol.14, no.2, pp. 169-168, June 2014.
[7] Y. Djeriri, A. Meroufel, A. Massoum and Z. Boudjema, Direct power control of a doubly fed induction generator based wind energy conversion systems including a storage unit, Journal of Electrical Engineering, JEE, Romania, vol.14, No.1, pp. 196-204, March 2014.
[8] C. Belfedal, S. Moreau, G. Champenois, T. Allaoui and M. Denai, Comparison of PI and Direct Power Control with SVM of Doubly Fed Induction Generator, Istanbul University, Journal of Electrical and Electronics Engineering, vol. 8, no. 2, pp. 633-641, 2008.
[9] M. V. Kazemi, A. S. Yazdankhah, H. M. Kojabadi, Direct power control of DFIG based on discrete space vector modulation, Elsevier, Renewable Energy, vol. 35, no. 5, pp. 1033-1042, May 2010.
[10] G. Abad, M. A. Rodriguez, J. Poza, Two-level VSC-based predictive direct power control of the doubly fed induction machine with reduced power ripple at low constant switching frequency, IEEE Trans. Energy Convers., vol. 23, no. 2, pp. 570-580, June 2008.
[11] D. Zhi, L. Xu, B. W. Williams, Model-Based Predictive Direct Power control of Doubly Fed Induction Generator, IEEE Trans.on .Power Electronics, vo1.25, no.2, pp. 341-351, February 2010.
[12] M. V. Kazemi, M. Moradi, R. V. Kazemi, Minimization of powers ripple of direct power controlled DFIG by fuzzy controller and improved discrete space vector modulation, Elsevier, Electric Power Systems Research, vol. 89, pp. 23-30, March 2012.
[13] M. Pichan, H. Rastegar, M. Monfared, Two fuzzy-based direct power control strategies for doubly-fed induction generators in wind energy conversion systems, Elsevier, Energie, vol. 51, pp. 154-162, February 2013.
[14] R. A. De Marchi, F. J. Von Zuben, E. Bim, A Neural Network Approach for the Direct Power Control of a Doubly Fed Induction Generator, XI Brazilian Congress of Power Electronics, IEEE, vol. 1, pp.38-43, Natal, Brasil, Sept. 2011.
[15] B. Hopfensperger, D.J. Atkinson and R. Lakin, Stator-Flux-Oriented Control of a Doubly-Fed Induction Machine with and without Position Encoder, IEE Proceedings -Electric Power Applications, vol. 147, no. 4, pp. 241-250, 2000.
[16] J.J. Moré, The Levenberg-Marquardt Algorithm: Implementation and Theory, Numerical Analysis, ed. G. A. Watson, Lecture Notes in Mathematics 630 , Springer Verlag, pp.105-116, 1977.
[17] M.T. Hagan, M. Menhaj, Training feedforward networks with the Marquardt algorithm, IEEE Trans, Neural Networks, vol. 5, no. 6, pp .989-993, 1994.

Appendix

Table I. Wind turbine parameters

Blade radius, R	35.25 m
Number of blades	3
Gearbox ratio, G	90
Moment of inertia, J	1000 Kg.m^2
Viscous friction coefficient, f_r	0.0024 N.m.s^{-1}
Cut-in wind speed	4 m/s
Cut-out wind speed	25 m/s
Nominal wind speed, v	16 m/s

Table II. Doubly fed induction generator parameters

Rated power, P_n	1.5 MW
Stator rated voltage, V_s	398/690 V

Rated current, I_n	1900 A
Stator rated frequency, f	50 Hz
Stator inductance, L_s	0.0137 H
Rotor inductance, L_r	0.0136 H
Mutual inductance, L_m	0.0135 H
Stator inductance, R_s	0.012 Ω
Rotor inductance, R_r	0.021 Ω
Number of pair of poles, p	2